

# Meteorological factors driving glacial till variation and the associated periglacial debris flows in Tianmo Valley, southeast Tibetan Plateau

M. F. Deng<sup>1,2</sup>, N. S. Chen<sup>1\*</sup>, and M. Liu<sup>1,2</sup>

(<sup>1</sup>Key Laboratory of Mountain Hazards and Surface Process, Institute of Mountain Hazards and Environment, Chinese Academy of Sciences, Chengdu 610041, China;

<sup>2</sup> University of Chinese Academic of Sciences, Beijing 100049, China)

Abstract: Meteorological studies have indicated that high alpine environments are strongly affected by climate warming, and periglacial debris flows are frequent in deglaciated regions. The combination of rainfall and air temperature controls the initiation of periglacial debris flows, and the addition of meltwater due to higher air temperatures enhances the complexity of the triggering mechanism compared to that of storm-induced debris flows. On the southeastern Tibetan Plateau, where temperate glaciers are widely distributed, numerous periglacial debris flows have occurred over the past 100 years, but none occurred in the Tianmo watershed until 2007. In 2007 and 2010, three large-scale debris flows occurred in the Tianmo Valley. In this study, these three debris flow events were chosen to analyse the impacts of the annual meteorological conditions, including the antecedent air temperature and meteorological triggers. The remote sensing images and field measurements of the adjacent glacier suggested that sharp glacier retreats occurred in the one to two years preceding the events, which coincided with spikes in the mean annual air temperature. Glacial till changes providing enough active sediment driven by a prolonged increase in the air temperature are a prerequisite of periglacial debris flows. Different factors can trigger periglacial debris flows, and they may include high intensity rainfall, as in the first and third debris flows, or continuous, long-term increases in air temperature, as in the second debris flow event.

Key words: glacial till variation; meteorological factors; periglacial debris flows; southeast Tibetan Plateau

## 1. Introduction

Alpine environments are vulnerable to climate changes, and alpine glaciers and permafrost are the most sensitive to degradation (Harris et al., 2009; IPCC, 2013). Glacier and permafrost retreat can induce mass movements such as landslides, shallow slides, debris slides, moraine collapses, etc. (Cruden and Hu, 1993; Korup and Clague, 2009; McColl, 2012; Stoffel and Huggel, 2012; Fischer et al., 2012). These movements would bring the material out of the watersheds in the form of debris

32 flows or sediment fluxes. Debris flows in alpine regions often bury residential areas,  
33 cut off main roads, block rivers (Shang et al., 2003; Cheng et al., 2005; Deng et al.,  
34 2013) and destroy basic facilities downstream; thus, they pose a considerable threat to  
35 the local economy and social development. In undeveloped alpine areas where the  
36 transportation system is particularly poor or limited, such as in southeastern Tibet, the  
37 negative effects produced by debris flows, such as cutting off main roads, can be  
38 serious (Cheng et al., 2005).

39 Periglacial debris flows occur in high alpine areas with large areas of glaciers,  
40 such as on the Tibetan Plateau in China (Shang et al., 2003; Ge et al., 2014), in the  
41 Alps in Europe (Sattler et al., 2011; Stoffel and Huggel, 2012), in the Caucasus  
42 Mountains in Russia (Evans et al., 2009) and in northern Canada (Lewkowicz and  
43 Harris, 2005). Periglacial debris flows can be initiated by rainfall (Stoffel et al., 2011;  
44 Schneuwly-Bollschweiler and Stoffel, 2012), glacial meltwater flow or ice particle  
45 ablation (Arenson and Springman, 2005; Decaulne et al., 2005) or outburst floods  
46 from glacier lakes (Chiarle et al., 2007) in different parts of the world; however,  
47 multiple triggers of a single event have rarely been studied. Because debris flows are  
48 commonly triggered by rainfall (Sassa and Wang, 2005; Decaulne et al., 2007; Kean  
49 et al., 2013; Takahashi, 2014), the rainfall threshold, intensity and duration have been  
50 widely used for debris flow monitoring and to provide event warnings in non-glacier  
51 areas (Guzzetti et al., 2008).

52 In deglaciaded areas, the debris flow threshold can be more difficult to determine.  
53 Periglacial debris flows tend to occur in the summer when the thawing of glaciers and  
54 glacial tills predominates and meltwater penetrates the glacial tills at a constant and  
55 successive flow rate. The effect of meltwater is similar to that of antecedent rainfall  
56 (Rahardjo et al., 2008) and is variable in different periods, considering snow and  
57 glacier shrinkage and air temperature fluctuations. In the Swiss Alps, the meltwater  
58 volume is high in early summer, and debris flows can be initiated by low intensity  
59 rainfall. However, larger rainstorms are required to produce debris flows in late  
60 summer and early autumn when the meltwater volume is low (Stoffel et al., 2011;  
61 Schneuwly-Bollschweiler and Stoffel, 2012). On the southeastern Tibetan Plateau, the

62 rainfall threshold given by Chen et al. (2011) is relatively wide (0.2~2.0 mm/10min,  
63 0.6~6.3 mm/h or 3.0~19.4 mm/24h), the small rainfall threshold of which is likely  
64 affected by the air temperature. Moreover, periglacial debris flows induced by sudden  
65 releases of water from glacier lakes are closely related to increasing air temperature  
66 (Liu et al., 2014).

67 Air temperature fluctuations are likely important triggers of periglacial debris  
68 flows. Compared to storm-induced debris flows, the addition of meltwater due to  
69 increased air temperature can greatly enhance the complexity of the initiation  
70 mechanism of periglacial debris flows. It is difficult to simulate the triggering process  
71 via experiments or mathematical simulation; thus, case studies of natural debris flows  
72 must be explored. In this study, three debris flow events in the Tianmo watershed on  
73 the southeastern Tibetan Plateau are used as examples after a debris flow-free period  
74 of nearly 100 years as deglaciation continues. The annual meteorological conditions,  
75 antecedent air temperature and triggering conditions prior to debris flows are analysed  
76 to further understand the meteorological triggers and their roles in glacier retreat,  
77 glacial till variation and debris flow initiation.

## 78 **2. Background**

### 79 **(1) Study area**

80 Temperate glaciers on the Tibetan Plateau are primarily distributed in the Parlung  
81 Zangbo Basin, and they covered a total landmass of 2381.47 km<sup>2</sup> in 2010 based on  
82 TM images (taken by the No. 4 or 5 thematic mappers on the Landsat satellite with a  
83 spatial resolution of 30 m) (Liu, 2013). Historically, the movement of temperate  
84 glaciers has produced numerous moraines, the depth of which can reach 500 m locally  
85 (Yuan et al., 2012). In recent decades, a significant temperature increase has occurred,  
86 and the temperature at the Bomi meteorological station (central Parlung Zangbo Basin)  
87 increased by 0.23°C/10a from 1969 to 2007, resulting in remarkable glacial shrinkage  
88 (Yang et al., 2010).

89 Tianmo Valley, which is located in Bomi County and to the south of the Parlung

90 Zangbo River, covers an area of 17.76 km<sup>2</sup> (29°59'N/95°19'E; Figure 1). This valley  
91 has a northeast-southeast orientation and is surrounded by high mountains reaching  
92 5590 m a.s.l. at the southernmost location and 2460 m a.s.l. at the fork in the Parlung  
93 Zangbo River. The TM image from 2013 illustrated the presence of a hanging glacier  
94 with an area of 1.42 km<sup>2</sup> in the upper concave area at an elevation of 4246 m to 4934  
95 m. Bare rock, dipping at an angle of approximately 60°, emerges below and above the  
96 hanging glacier and is often covered by snow. Below 3800 m a.s.l., vegetation,  
97 including forest and shrubs, occupies most of the area (Table 1).

98 The river channel in the watershed is sheltered by shade and not directly affected  
99 by sunlight, resulting in less solar radiation and a location at which a small trough  
100 glacier can form. In the main channel, the trough glacier extended to 2966 m a.s.l. in  
101 2006. The lower part of the trough glacier has been eroded by glacier meltwater flow,  
102 and an arch glacier that is vulnerable to high pressure was formed (Figure 2). The  
103 remnants of the landslide deposits are approximately 10 metres high can be observed  
104 on both sides of the channel. These deposits consist of low-stability sediment and can  
105 be easily entrained by debris flows.

106 Tianmo Valley is located on the north side of the bend in the Yarlung Zangbo  
107 River and is strongly affected by new tectonic movement. An inferred normal fault  
108 vertical to the channel cuts through the valley and is only 30 km from the Yarlung  
109 Zangbo fault. In 1950, a rather significant earthquake (Ms. 8.6) hit Zayu, which is  
110 only 200 km away, and local records reported that a large amount of rock collapsed  
111 and landslides were produced at that time. The whole valley is located in a strong  
112 ductile deformation zone and is dominated by gneissic lithology belonging to a  
113 Presinian System.

## 114 **(2) Disaster history**

115 According to our field interviews with local residents, there were no debris flows  
116 in the approximately 100 years prior to 2007 in Tianmo Valley. The channel was  
117 relatively narrow before 2007, and the local people could walk across via a wooden  
118 bridge to live and farm on the terrace on the west side. On the morning of September

119 4<sup>th</sup>, 2007, a rainfall even hit this area and it ceased around 7:00. On the evening of  
120 approximately 18:00, the local forest guard heard a loud noise coming from the  
121 upstream area and rainfall later began in the upstream area at approximately 19:00.  
122 Then, debris flows occurred in the Tianmo Channel after the second rainfall event,  
123 and they subsequently blocked the Parlung Zangbo River. It is told by the local citizen  
124 that several debris flows occurred during that entire night while we cannot separate  
125 them according to the field measurements, and approximately 1,340,000 m<sup>3</sup> of  
126 sediment was transported during this event, resulting in 8 missing persons and deaths.  
127 This debris flow event is listed as DF1 in this paper, which contained the first debris  
128 flows and the following waves. Concurrently, debris flows occurred in the four  
129 adjacent 4 valleys (Table 2). According to the size classification proposed by Jakob  
130 (2005), which is based on the total volume, peak discharge and inundated area, the  
131 size classes of the debris flows in the five valleys are given in Table 2.

132 At 11:30 on July 25<sup>th</sup>, 2010, debris flows were again triggered in Tianmo Valley  
133 that traced the path of the preceding debris flow deposits and reached the other side of  
134 the Parlung Zangbo River. According to Ge et al. (2014), a solid sediment mass of  
135 approximately 500,000 m<sup>3</sup> was carried to (Table 1) and deposited in the channel and  
136 blocked the main river. A barrier lake was formed, and the rising water destroyed the  
137 roadbed of G318. Dozens of small-magnitude debris flows occurred in the following  
138 week. This debris flow event is listed as DF2 in this paper and it contained several  
139 waves.

140 Debris flows occurred again two months later on Sep. 6<sup>th</sup> (The Ministry of Land  
141 and Resources P. R. C., 2010), although we could not determine the exact time  
142 sequence of the events. According to speculation, the debris flows could have  
143 occurred in the early morning before dawn when the rainfall intensity reached its  
144 maximum (Figure 9). This theory agrees with the findings of Chen (1991), who found  
145 that periglacial debris flows historically occurred between 18:00~24:00 in this area.  
146 The debris barrier in the main river was consequently increased by an additional  
147 450,000 m<sup>3</sup>, and the barrier lake was enlarged to hold 9,000,000 m<sup>3</sup> of water. This  
148 debris flow event is listed as DF3 in this paper and waves of which cannot be

149 determined.

150 A field investigation revealed that a high percentage of boulders in the  
151 downstream area and glacial tills above the trough glacier are loose and high porosity  
152 rocks (Figure 2); hence, they have low density and can be easily entrained. Our  
153 particle size tests of the glacial tills and debris flow deposits indicate a low clay  
154 ( $d < 0.005$  mm) content, whereas the debris flow deposits contain more fine particles  
155 that are smaller than 10 mm (Figure 4), suggesting that entrainment accounted for a  
156 considerable amount of fine particles.

### 157 **(3) Meteorological data**

158 The study area is located in a high alpine area where the economy is relatively  
159 undeveloped and few meteorological stations exist. Before 2011, the Bomi  
160 meteorological station (established in 1955) was the only station in the area. It is  
161 located 54 km from Tianmo Valley at an elevation of 2730 m, and other stations were  
162 located more than 200 km away.

163 The Tibetan Plateau is a massive terrace that obstructs the Indian monsoon,  
164 causing it to travel through the Yarlung Zangbo Canyon and its tributaries. As the  
165 Indian monsoon is transported to higher altitudes, a rainfall gradient emerges in the  
166 Parlung Zangbo Basin. However, according to the rainfall data from the area, rainfall  
167 often exhibits a similar intensity as that of the long-term rainfall process from  
168 Guxiang to Songzong, which suggests that a large rainfall gradient does not exist  
169 between Tianmo Valley and Bomi meteorological station; therefore, the rainfall data  
170 from Bomi meteorological station could be used in our study. To conduct additional  
171 studies, another meteorological station was built in 2011 near Tianmo Valley.

172 It has been established that the air temperature decreases with altitude; therefore,  
173 the air temperature in the source area of Tianmo Valley is lower than that in Bomi  
174 County. According to the research by Li and Xie (2006), the air temperature decreases  
175 at a rate of  $0.46\sim 0.69^{\circ}\text{C}/100$  m over the entire Tibetan Plateau, and the rate in the  
176 study area is  $0.54^{\circ}\text{C}/100$  m. Because the glacier and permafrost in the source area  
177 have planar distributions, the air temperature at the geometric centre of the glacier and

178 permafrost can be used to analyse the temperature process.

### 179 **3. Analysis and results**

#### 180 **(1) Air temperature and rainfall changes**

181 The mean annual air temperature is generally used to reflect the trends of glacier  
182 change (Yang et al., 2015). We collected mean annual air temperature and annual  
183 rainfall data from 1970 to 2014 from the Bomi meteorological station (Figure 5). The  
184 records showed that the mean air temperature has increased by approximately 1.5 °C  
185 over the past 45 years at a rate of 0.033 °C/a. This air temperature increase was  
186 particularly rapid between 2005 and 2007 at approximately 0.7 °C/3a, which is 7  
187 times the average value over the past 45 years. However, the annual rainfall from  
188 2000 to 2010 was low and estimated as 828.2 mm per year. From 2000 to 2004, the  
189 rainfall during summer (July to September) accounted for approximately 50% of the  
190 total annual rainfall; however, only 32% of the rainfall occurred in the summer of  
191 2005~2006, even though the annual rainfall exhibited a similar trend. In 2007, rainfall  
192 in the summer and the entire year returned to the mean rainfall state.

193 Figure 5 shows similar air temperature and rainfall trends before DF2 and DF3.  
194 The air temperature increased in 2009 and reached 10.2 °C which is the maximum of  
195 the past 45 years; however, the annual rainfall went down to only 65% of the average  
196 amount; and the summer rainfall reached a minimum value. In 2010, rainfall was  
197 abundant, and the annual rainfall increased to 1080.6 mm, which is approximately 30%  
198 more than the average value and close to the maximum.

199 The following common traits can be identified by comparing the annual  
200 meteorological conditions of DF1, DF2 and DF3: 1) one or two years before the  
201 debris flows, the mean annual temperature increased and the annual rainfall and  
202 summer rainfall decreased. Additionally, the climate was in a "hot-dry" state; 2) As  
203 the temperature gradually decreased, the annual rainfall returned to normal or  
204 increased, and a "hot-wet" climate state contributed to debris flow initiation (Lu and  
205 Li, 1989).

## 206 (2) Changing of glacier in Tianmo Valley

207 In our study, remote images were collected to analyse the glacier changes in the  
208 source area in recent years. To eliminate the effect of snow cover, images were taken  
209 in the thawing seasons when snow cover is limited, enabling easy detection of glaciers  
210 and snow. Moreover, an image taken on a bright, cloudless day is still needed to show  
211 the watershed clearly; however, a difficult case is encountered when the rainy season  
212 begins during the thawing season, as the atmosphere is often covered by thick clouds.  
213 Furthermore, to illustrate glacier retreat and its impact on debris flows properly, the  
214 images should be within similar time intervals, such as 3 years, before and after debris  
215 flow events. High-resolution images are rare, and we could only collect one SPOT  
216 image (taken by the Systeme Probatoire' Observation de la Terre satellite with a  
217 spatial resolution of 5 m) in 2008. To achieve image consistency, we collected 5 TM  
218 images taken on September 17<sup>th</sup>, 2000, July 24<sup>th</sup>, 2003, September 21<sup>st</sup>, 2006,  
219 September 24<sup>th</sup>, 2009 and August 4<sup>th</sup>, 2013.

220 Based on the 5 TM images, we classified the area as glacier, snow, bare land,  
221 gully deposit and vegetation in time series (Figure 6), and the area of each is given in  
222 Table 1. Figure 6 shows that deglaciation occurred in Tianmo Valley; notably, the  
223 eastern branch has experienced considerable deglaciation. To clearly show the rapid  
224 rate of glacial retreat in the entire basin and eastern branch, a graph of retreat was  
225 plotted, as shown in Figure 7.

226 Figure 7 shows that the glacier in Tianmo Valley shrank from 2000 to 2013, with  
227 variable rates of glacier retreat. In 2000~2003, 2003~2006, 2006~2009 and  
228 2009~2013, the glacier retreat rates in Tianmo Valley were 0.02, 0.06, 0.027 and  
229 0.0075 km<sup>2</sup>/a, respectively, and those of the eastern branch were 0.0033, 0.01, 0.008  
230 and 0.002 km<sup>2</sup>/a, respectively. According to the figure, the largest glacier retreat rate  
231 was observed in 2003~2006, followed by that in 2006~2009. The glacier area at the  
232 beginning should be noted to assess the rate of change of the glacier. The glacier  
233 retreat rate can be normalized, and the relative glacier retreat rate can be calculated  
234 based on this change in area.



235 The relative glacier retreat rates were 11.30, 35.09, 17.43 and  $5.17 \times 10^{-3} \text{km}^2/\text{a}/\text{km}^2$   
236 in 2000~2003, 2003~2006, 2006~2009 and 2009~2013, respectively; and the  
237 corresponding values were 20.83, 66.67, 66.67 and  $20.83 \times 10^{-3} \text{km}^2/\text{a}/\text{km}^2$  for the  
238 eastern branch. The relative glacier retreat rate of the eastern branch decreased sharply  
239 between 2000 ~2013.

240 In this study, TM images over 3-year intervals were applied to obtain the mean  
241 glacier retreat rate. As glacier retreat rate in the 3 three years could be either high or  
242 low, field measurements of the nearby glacier were used to show the glacier retreat  
243 condition before debris flows occurred. Yang et al. (2015) conducted field  
244 measurements of the No.94 Glacier in the Parlung Zangbo Basin since 2006, and the  
245 field measurements suggest it had a negative balance from 2006~2010 (Figure 7). The  
246 negative balance reached a maximum level in 2009, followed by 2008 and 2006,  
247 indicating rapid deglaciation in these three years.

248 When we combined the results of the TM image analysis and field measurements  
249 of the No. 94 Glacier, we observed that the glacier in Tianmo Valley experienced the  
250 most rapid deglaciation prior to debris flows in 2006, 2008 and 2009, which coincided  
251 with an increase in the mean annual air temperature (Figure 5). Moreover, the  
252 maximum glacier retreat in 2009 was potentially related to the decline in snowfall in  
253 the preceding winter and early spring.

### 254 **(3) Antecedent air temperature and rainfall**

255 The air temperature in the source area can be obtained based on a vertical rate of  
256 decline ( $0.54 \text{ }^\circ\text{C}/100 \text{ m}$ ). Based on this method, the air temperature in the source area  
257 was  $9.8 \text{ }^\circ\text{C}$  lower than that at the Bomi meteorological station. We collected the  
258 lowest temperature, the mean temperature and daily rainfall from June to September  
259 in 2007 and 2010 (Figure 8).

260 Figure 8 shows that the lowest air temperature was below 0 at the end of June  
261 2007. At the beginning of July, the air temperature started to rise quickly, which  
262 continued until early September when DF1 occurred. This trend suggests that the high  
263 air temperatures in July and August contributed to DF1.

264 Additionally, the air temperature was high from early July to late August, and  
265 another high air temperature period was observed in early September. When DF2  
266 occurred in late July, the air temperature had reached the maximum for that year,  
267 which suggests that the air temperature in early and mid-July was responsible for DF2.  
268 After DF2 occurred, the air temperature in August varied towards the conditions that  
269 caused DF3.

270 Antecedent air temperature fluctuations include the air temperature and the  
271 duration of variations. The air temperatures and durations before debris flows are  
272 variable and difficult to evaluate. The accumulation of positive air temperature is  
273 often used to analyse the effect of air temperature on glacier melting (Rango and  
274 Martinec, 1995) and can be expressed as follows:

$$275 \quad T_{PT} = \sum_{i=-n}^0 T_i (T_i > 0) \quad (1)$$

276 where  $T_{PT}$  is positive air temperature accumulation (°C) and  $T_i$  is the average  
277 daily air temperature (only  $T_i > 0$  is included).

278 Because air temperature is successive, it is difficult to determine the beginning of  
279 positive air temperature accumulation. Glacial tills can decrease the heat that  
280 penetrates into them, and the low air temperature is only observed in the upper thin  
281 layer. Moreover, freeze-thaw cycles exist when the lowest air temperature is less than  
282 0°C. From this perspective, the beginning of positive air temperature accumulation is  
283 defined as the time at which the lowest air temperature exceeds 0°C for two or three  
284 successive days or since the last debris flow.

285 Based on the above method, we can deduce that positive air temperature  
286 accumulation began when the lowest air temperature exceeded 0°C for several  
287 successive days beginning on June 28<sup>th</sup>, 2007, June 9<sup>th</sup>, 2010, and July 26<sup>th</sup>, 2010,  
288 which correspond to DF1, DF2 and DF3, respectively. The duration and  $T_{PT}$  were  
289 calculated for each debris flow event. The results were 69 days and 517.9 °C, 47 days  
290 and 332.1 °C and 42 days and 320.4 °C (Figure 8) for DF1, DF2 and DF3,

291 respectively. The results showed that  $T_{PT}$  for DF1 was much larger than the other  
292 two  $T_{PT}$  values, which coincides with the fact that there were no debris flows in the  
293 past dozens of years, and extraordinary external forces such as large  $T_{PT}$  are required  
294 to disrupt the long-term balance.

#### 295 **(4) Triggering conditions**

296 Rainfall in a short can trigger debris flows while it cannot be triggered by a sole  
297 abrupt increase in air temperature as the continuous and limited nature of air  
298 temperature, instead, air temperature of longer term should be included. In our  
299 analysis, the rainfall over the three days preceding a debris flow event is given in  
300 Figure 9.

301 Before DF1, the air temperature was high, which continued through July and  
302 August. Notably, the  $T_{PT}$  reached 517.9°C. According to the local forest guard, an  
303 isolated convective storm occurred prior to DF1, although no rainfall was recorded at  
304 the Bomi meteorological station or in the downstream area at that time. In Figure 9, as  
305 the rainfall right before DF1 occurred was not recorded by the Bomi metrological  
306 station, we added approximately 5 mm/h of rainfall intensity (according to the  
307 description provided by the forest guard) before DF1 to account for the storm, which  
308 might not reflect the real rainfall process. We can therefore conclude that this isolated  
309 convective storm initiated DF1, while the long-term high air temperature trend paved  
310 the way for DF1. Considering a large deglaciated area, several other periglacial debris  
311 flows simultaneously occurred near Tianmo Valley (Deng et al., 2013), which  
312 suggests the advantageous meteorological conditions for debris flow initiation.

313 DF2 occurred when the air temperature reached a peak in 2010. The thaw season  
314 began in the middle of June, and  $T_{PT}$  reached 332.1 °C. On July 24<sup>th</sup>, one day before  
315 DF2, the air temperature reached a maximum value for that year. No rainfall event hit  
316 this area preceding DF2 according to the record of Bomi meteorological station, and  
317 the local citizens also observed no rain. The trigger of DF2 was likely the continuous

318 percolation of meltwater due to the long-term increase in air temperature.

319 According to field interviews, several debris flows of small magnitude occurred  
320 before DF3. The air temperature decreased in late August but increased to another  
321 high value before DF3, and the  $T_{PT}$  reached 320.4 °C. Rainfall began 2 days prior to  
322 DF3 and lasted the entire day before DF3. According to the rainfall trend at the Bomi  
323 meteorological station, the rapid increase in rainfall intensity started 4 hours before  
324 DF3 and reached 3.8 mm/h, which was responsible for the initiation of DF3.

## 325 **4. Discussion**

326 In this study, we found that the triggering factors of the three debris flows were  
327 high air temperature and rainfall for DF1, high air temperature for DF2 and storm for  
328 DF3, respectively. When we analysed the dates and triggers of these events, various  
329 questions should be settled first: 1) why did debris flows not occur in 2006 or 2009  
330 when deglaciation reached its peak and more ice meltwater was present; 2) why did  
331 DF1 and DF3 occur in September when the air temperature and volume of ice  
332 meltwater were decreasing; and 3) why there were no large-scale debris flows  
333 triggered by previous heavy storms. Based on our results, we believe that the impact  
334 of the water source on the magnitude and frequency of debris flows is relatively small,  
335 or more debris flows would form during the early larger storm; instead, the sediment  
336 source, including the associated magnitude and activity, may be the predominant  
337 control, as reported by Jakob et al. (2005), who noted that channel recharge is a  
338 prerequisite for debris flows. However, in most situations, we cannot reach the source  
339 area to detect the soil source, and high-tech remote sensing can only distinguish the  
340 boundary of the soil source. In the periglacial area where glacial till is often covered  
341 by glacier or everlasting snow, a change in the soil source would be highly difficult to  
342 detect. In this study, we combine the meteorological conditions and literature reports  
343 to discuss the likely variations in glacial tills before debris flows.

### 344 **(1) Annual variations in glacial till**

345 Climate warming is a global trend (IPCC, 2013), and the Tibetan Plateau, as the

346 third pole, is no exception to climate change. According to our statistics, the air  
347 temperature in Bomi County has increased by 1.5 °C over the past 45 years  
348 (1970~2014). Glacier retreat induced by climate warming has been widely accepted,  
349 and recent research suggests that the weaker Indian monsoon could be another reason  
350 for such retreat (Yao et al., 2012). Glaciers are always located in concave ground  
351 areas and cover large volumes of glacial tills. Glacial pressure can generate normal  
352 stress vertical to the slope, which can strengthen the slope stability. The effect of  
353 glaciers on slope stability is called glacial debuttrressing (Cossart et al., 2008). As  
354 deglaciation continues, the result could lead to the exposure of the frozen glacial tills  
355 (Figure 10 A to B) and smaller glacial debuttrressing.

356 The retreats of glaciers and glacial tills due to climate warming are quite  
357 different. The newly formed bare glacial till is frozen with a high ice content. The  
358 cohesion of the ice particles creates a bare glacial till with high shearing strength and  
359 stability. Deglaciation is accompanied by the melting of internal ice particles, which  
360 can greatly enhance the activity. This process first occurred at the surface layer of  
361 glacial till, followed the layers below, resulting in enlargement of active debris. As the  
362 debris obstruct heat fluxes from penetrating into the layer below, so the melting rate of  
363 internal ice particles is quite slower than that of glacial retreat (Takeuchi et al., 2000),  
364 result into a strong heat gradient at the surface while limited in deep layers, which  
365 means the activity of the debris decline with depth and long term high air temperature  
366 is required to enhance the activity in a deeper layer. As the ablation rates is quite low,  
367 only the surface layer is highly active and the sediment is relatively limited. Therefore,  
368 no debris flows of large magnitude could occurred in 2006 and 2009 when glacier  
369 retreat reached a maximum while the active glacial till is restricted to the surface  
370 layer.

## 371 **(2) Variation in glacial till on antecedent days**

372 After the long, cold winter, glacial tills become frozen. If a regressive glacier  
373 does not recover in the winter, glacial tills are covered by snow. As the air temperature  
374 increases again, the surface snow melts first, followed by the internal ice particles.

375 The thawing of internal ice particles induces a series of changes in the glacial till,  
376 which include the following: 1) the thawing will break the bonds of ice particles and  
377 increase the instability between ice cracks (Ryzhkin and Petrenko, 1997; Davies et al.,  
378 2001); 2) the sharp air temperature fluctuations in high alpine, mountainous areas  
379 induce a repeated cycle of expansion and contraction in the glacial till that can destroy  
380 the mass structure to some extent; 3) the seepage of ice meltwater can transport  
381 fine-grained sediments that were formerly frozen in the ice matrix (Rist, 2007); and 4)  
382 the ice meltwater can result in a higher water content and pore water pressure  
383 (Christian et al., 2012). These changes in glacial till can sharply decrease the soil  
384 strength, shifting to an active mass from an uncovered and frozen moraine (Figure  
385 10B to C). Because heat conduction in glacial till is relatively slow, this process may  
386 last for a very long time and require a high antecedent air temperature.

387 Heat conduction via the percolation of rainfall and ice meltwater can amplify the  
388 depth of active glacial till (Gruber and Haeberli, 2007), whereas covering the surface  
389 glacial till can hinder a heat flux from penetrating into the deep layers (Noetzli et al.,  
390 2007). At a low air temperature, the heat flux should be constrained to the surface  
391 layer, and a large heat gradient due to a high air temperature would contribute much  
392 more to the heat flux and ice melt in the deep mass. Thus, the long-term effect of a  
393 high air temperature can amplify the active glacial till (Noetzli et al., 2007; Åkerman  
394 and Johansson, 2008), under which lies frozen glacial till with a high ice content. The  
395 activity of glacial till varies with depth from high at the surface to low in the deep  
396 layers, and landslide failure can take place on glacial till slopes in a retrogressive  
397 manner, coinciding with long-term air temperature fluctuations, as active glacial till is  
398 relatively limited in deglaciated areas.

### 399 **(3) Failure of glacial till**

400 Different factors can lead to glacial till failure. Active glacial till slopes with low  
401 strength are usually vulnerable, and their failure can occur when the air temperature is  
402 above 0 °C (Arenson and Springman, 2005). Rainfall or ice melt water induced by air  
403 temperature can trigger the failure (Figure 10 C to D). This type of event is called a

404 shallow landslide, and the failure mechanism lies in the ablation of internal ice  
405 particles and the percolation of meltwater, which can initially decrease the soil  
406 strength (Arenson and Springman, 2005; Decaulne et al., 2005). Later, the subsequent  
407 rapid percolation of ice meltwater or heavy rainfall can saturate the debris, decrease  
408 soil suction and shearing strength, and form seepage flows that can trigger the shallow  
409 landslide failure (Springman et al., 2003; Decaulne and Sæmundsson, 2007; Chiarle et  
410 al.,2007). Whether the failure can induce debris flows is still dependent on its ability  
411 to entrain the debris layer as the flow moves through the channel.

412 Another type of failure might take place when peaked runoff flows over and  
413 entrains debris deposits in the charged channel and reach a critical discharge (Berti  
414 and Simoni, 2005; Gregoretto and Dalla Fontana, 2008; Kean et al., 2012, 2013;  
415 Takahashi, 2014; Rengers et al., 2016, Gregoretto et al., 2016), which is more  
416 determined by channel bed slope and grain size of debris (Tognaccaet al., 2000;  
417 Gregoretto, 2000; Theule et al., 2012; Hurlimann et al., 2014; Degetto et al., 2015).  
418 This type of channelized runoff could be a combination of three factors: rainfall,  
419 melting ice or the overflow that forms when a glacier collapses downward into a  
420 water pool. Mechanism of this process lies in the hydrodynamic forces exerted on the  
421 surface elements of debris layers and surpassing sediment resistance (Gregoretto and  
422 Dalla Fontana, 2008; Recking et al., 2009; Prancevic et al., 2014). FaThe  
423 concentration of runoff in the channel bottom causes the erosion of the debris surface  
424 layer forming a solid-liquid current at first, then extends to the layers below with  
425 whole or partial mobilization and debris flows was generated (Gregoretto and Dalla  
426 Fontana, 2008). Therefore, debris flows initiated by landslide failure caused by  
427 seepage flow or channelized runoff that entrain sediments in the periglacial area is  
428 similar with the mechanism of debris flows initiation in non-glacier areas (Iverson et  
429 al., 1997; Springman et al., 2003; Sassa and Wang, 2005; Gregoretto and Dalla  
430 Fontana, 2008; Kean et al., 2013), while the difference lies in the activity of debris  
431 and the source of water. In the European Alps, periglacial debris flows are mainly  
432 provoked by rainfall, which is also related to air temperature fluxes (Stoffel et  
433 al.,2011). Additionally, the values of rainfall and air temperature required to trigger

434 debris flows could be inversely correlated. Air temperature increases can cause  
435 melting and water runoff; thus, the rainfall required to create percolation flows or  
436 critical discharge to trigger a debris flow would be much less. In addition, the  
437 intensity and duration of the required rainfall may require other preconditions, such as  
438 those associated with the distributions of glaciers and frozen glacial tills and the  
439 terrain of the source area, to enhance the debris flow (Lewkowicz and Harris, 2005).

440 The three debris flow events were associated with similar annual meteorological  
441 conditions, except that the positive air temperature accumulation prior to DF1 was the  
442 largest. DF1 occurred at the end of a prolonged period of high air temperature, prior to  
443 this, there were instances of small failures but no large-scale debris flows. On July  
444 25<sup>th</sup>, 2007, the daily rainfall reached 20.7 mm, while no debris flows were generated  
445 because the active glacial till is restricted in the shallow surface layer after a short  
446 term of air temperature increase.

447 In 2010, the largest daily rainfall occurred on June 7<sup>th</sup>, accounting for 37.5 mm,  
448 at the beginning of an air temperature increase when the glacial till was frozen with  
449 low activity. The lack of glacial till with high activity was the likely cause of the  
450 absence of debris flows. The similar situation could be found on August 23<sup>rd</sup> when the  
451 daily rainfall was 20.3 mm and the positive air temperature accumulation is low since  
452 DF2, which had produced quite limited active glacial till. Besides, a low and positive  
453 air temperature was observed prior to September 6<sup>th</sup> when DF3 occurred, the  
454 boundary of active glacial till had been enlarged before; moreover, the high rainfall  
455 intensity could supplemented this lack of prolonged high air temperature and trigger  
456 debris flows.

## 457 **5. Conclusion**

458 Climate changes have serious effects in high mountainous areas, and the mass  
459 movement of sediments such as periglacial debris flows has become increasingly  
460 frequent. Prolonged increases in the mean annual air temperature are regarded as very  
461 favourable for periglacial debris flows. In particular, the annual “hot-dry” weather  
462 conditions one or two years prior were responsible for three debris flow events in



463 Tianmo Valley. Debris flows are generally not initiated in the year when the mean  
464 annual air temperature spikes, as the melting of internal ice particles lags behind the  
465 rate of glacial retreat resulting from a prolonged increase in air temperature.

466 Glacial till is unlimited in deglaciated areas, and its activity relies on glacial  
467 retreat and internal ice particle melting. Glacial till changes induced by increased air  
468 temperature are the first steps in forming periglacial debris flows compared to  
469 storm-induced debris flows in non-glacier areas. Glacial tills require a four-phase  
470 process prior to debris flow occurrence. In this process, the variation in air  
471 temperature drives the glacial till change, including causing glacier recession,  
472 producing bare glacial till and enhancing the glacial till activity. Debris flows can  
473 occur when a sufficient amount of active glacial till exists and rainfall-induced  
474 seepage or runoff is more likely to generate debris flows.

475 It is difficult to observe glacial till changes in source areas of debris flows, and  
476 the analysis of the phase conversion of glacial till in this study is based on the  
477 triggering conditions and other literature findings. Indeed, the meteorological  
478 conditions, such as the antecedent air temperature and meteorological triggers that  
479 drive the phase conversion, are partly coupled and difficult to distinguish.

480 **Acknowledgements:** This research was supported by the National Natural Science Foundation  
481 of China (grant nos. 41190084, 41402283 and 41371038) and the “135” project of IMHE, CAS.  
482 We wish to acknowledge the editors of the Natural Hazards and Earth System Science Editorial  
483 Office and the anonymous reviewers for their constructive comments, which helped us improve  
484 the contents and presentation of the manuscript.

## 485 **References**

- 486 Åkerman, H. J. and Johansson, M.: Thawing permafrost and thicker active layers in  
487 sub-Arctic Sweden, *Permafrost Periglac. Process.*, 19, 279-292, 2008.
- 488 Arenson, L. U. and Springman, S. M.: Mathematical descriptions for the behaviour of  
489 ice-rich frozen soils at temperatures close to 0 °C, *Can. Geotech. J.*, 42, 431-442,  
490 2005.

491 Berti, M., and Simoni, A.: Experimental evidences and numerical modelling of debris  
492 flow initiated by channel runoff. *Landslides*, 2(3), 171-182, 2005.

493 Bommer, C., Fitze, P. and Schneider, H.: Thaw-consolidation effects on the stability  
494 of Alpine talus slopes in permafrost, *Permafrost Periglac. Process.*, 23, 267-276,  
495 2012. doi:10.1002/ppp.1751.

496 Chen, N. S., Zhou, H. B., and Hu, G. S.: Development rules of debris flow under the  
497 influence of climate change in Nyingchi, *Adv. Clim. Change Res.*, 7, 412-417,  
498 2011. (In Chinese).

499 Chen, R.: Initiation and the Critical Condition of Glacial Debris Flow, Master thesis,  
500 Institute of Mountain Hazards and Environment, Chinese Academic of Sciences,  
501 P19, 1991.

502 Cheng, Z. L., Wu, J. S., and Geng, X.: Debris flow dam formation in southeast Tibet,  
503 *J. Mt Sci.*, 2, 155-163, 2005.

504 Chiarle, M., Iannotti, S., Mortara, G., and Deline, P.: Recent debris flow occurrences  
505 associated with glaciers in the Alps, *Glob. Planet. Change*, 56, 123-136, 2007.

506 Cossart, E., Braucher, R., Fort, M., Bourlès, D. L., and Carcaillet, J.: Slope instability  
507 in relation to glacial debuitressing in alpine areas (Upper Durance catchment,  
508 southeastern France): evidence from field data and  $^{10}\text{Be}$  cosmic ray exposure  
509 ages, *Geomorphology*, 95, 3-26, 2008.

510 Cruden, D. M. and Hu, X. Q.: Exhaustion and steady state models for predicting  
511 landslide hazards in the Canadian Rocky mountains, *Geomorphology*, 8,  
512 279-285, 1993.

513 Davies, M. C. R., Hamza, O., and Harris, C.: The effect of rise in mean annual  
514 temperature on the stability of rock slopes containing ice-filled discontinuities,  
515 *Permafrost Periglac. Process.*, 12, 137-144, 2001.

516 Decaulne, A. and Sæmundsson, T.: Spatial and temporal diversity for debris-flow  
517 meteorological control in subarctic oceanic periglacial environments in Iceland,  
518 *Earth Surf. Process. Landf.*, 32, 1971-1983, 2007.

519 Decaulne, A., Sæmundsson, T., and Petursson, O.: Debris flows triggered by rapid  
520 snowmelt in the Gleidarhjalli area, northwestern Iceland, *Geografiska Annaler*,  
521 87A, 487-500, 2005 .

522 Degetto, M., Gregoretti, C and Bernard, M. Comparative analysis of the differences  
523 between using LiDAR contour-based DEMs for hydrological modeling of  
524 runoff generating debris flows in the Dolomites. *Front. Earth Sci.*, 3,21, 2015.

525 Deng, M. F., Chen, N. S., Ding, H. T., and Zhou, C. C.: The hydrothermal condition  
526 of 2007 group-occurring debris flows and its triggering mechanism in Southeast  
527 Tibet, *J. Nat. Dis.*, 22, 128-134, 2013 (In Chinese).

528 Evans, S. G., Tutubalina, O. V., Drobyshev, V. N., Chernomorets, S. S., McDougall,  
529 S., Petrakov, D. A., and Hungr, O.: Catastrophic detachment and high-velocity  
530 long-runout flow of Kolka Glacier, Caucasus Mountains, Russia in 2002,  
531 *Geomorphology*, 105, 314-321, 2009.

532 Fischer, L., Purves, R. S., Huggel, C., Noetzli, J., and Haeberli, W.: On the influence  
533 of topographic, geological and cryospheric factors on rock avalanches and  
534 rockfalls in high-mountain areas, *Nat. Hazards Earth Syst. Sci.*, 12, 241-254,  
535 2012.

536 Ge, Y. G., Cui, P., Su, F. H., Zhang, J. Q., and Chen, X. Z.: Case history of the  
537 disastrous debris flows of Tianmo watershed in Bomi County, Tibet, China:  
538 some mitigation suggestions, *J. Mt. Sci.*, 11, 1253-1265, 2014.

539 Gregoretti, C.: The initiation of debris flow at high slopes: experimental results, *J.*  
540 *Hydraulic Res.*, 38, 83-88, 2000.

541 Gregoretti, C., and Dalla Fontana, G.: The triggering of debris flow due to  
542 channel-bed failure in some alpine headwater basins of the Dolomites: analyses  
543 of critical runoff, *Hydrol. Process.*, 22, 2248-2263, 2008.

544 Gregoretti, C., Degetto, M., Bernard, M., Crucil, G., Pimazzoni, A., De Vido G., Berti,  
545 M., Simoni, A. Lanzoni, S. Runoff of small rocky headwater catchments: Field  
546 observations and hydrological modeling. *Water Resources Research*. 52, 10,  
547 8138-8158, 2016.

548 Gruber, S., and Haeberli, W.: Permafrost in steep bedrock slopes and its  
549 temperature-related destabilization following climate change. *J. Geophys. Res.*,  
550 112, (F02S18), 2007.

551 Guzzetti, F., Peruccacci, S., Rossi, M., and Stark, C. P.: The rainfall intensity-duration  
552 control of shallow landslides and debris flows: an update, *Landslides*, 5, 3-17,  
553 2008.

554 Harris, C., Arenson, L. U., Christiansen, H. H., Etzelmüller, B., Frauenfelder, R.,  
555 Gruber, S., Haeberli, W., Hauck, C., Hölzle, M., Humlum, O., Isaksen, K., Kääh,  
556 A., Kern-Lütschg, M. A., Lehning, M., Matsuoka, N., Murton, J. B., Nötzli, J.,  
557 Phillips, M., Ross, N., Seppälä, M., Springman, S. M., and Vonder Mühll, D.:  
558 Permafrost and climate in Europe: monitoring and modelling thermal,  
559 geomorphological and geotechnical responses, *Earth Sci. Rev.*, 92, 117-171,  
560 2009.

561 Hurlimann, M., Abanco, C., Moya, J., Vilajosana, I. Results and experiences gathered  
562 at the Rebaixader debris-flow monitoring site, Central Pyrenees, Spain.  
563 *Landslides*. 11, 6, 939-953, 2014.

564 Intergovernmental Panel of Climate Change, Summary for Policymakers. Working  
565 Group I Contribution to the IPCC Fifth Assessment Report Climate Change  
566 2013: The Physical Science Basis, Cambridge University Press, Cambridge, UK,  
567 2013.

568 Iverson, R. M., Reid, M. E., and LaHusen, R. G., Debris-flow mobilization from  
569 landslides, *Annu. Rev. Earth Planet Sci.*, 25, 85-138, 1997.

570 Jakob, M., Bovis, M., and Oden, M.: The significance of channel recharge rates for  
571 estimating debris-flow magnitude and frequency, *Earth Surf. Proc. Land*, 30,  
572 755-766, 2005.

573 Jakob, M.: A size classification for debris flows, *Eng. Geol.*, 79, 151-161, 2005.

574 Kean, J. W., McCoy, S. W., Tucker, G. E., Staley, D. M., and Coe, J. A.:  
575 Runoff-generated debris flows: observations and modeling of surge initiation,  
576 magnitude, and frequency, *J. Geophys. Res. Earth Surf.*, 118, 2190-2207, 2013.

577 Kean J.W., Staley D.M., Leeper R.J., Schmidt K.M., Gartner J.E. A low-cost method  
578 to measure the timing of postfire flash floods and debris flows relative to  
579 rainfall. *Water Resources Research*, 48,5, W05516, 2012.

580 Korup, O. and Clague, J. J.: Natural hazards, extreme events, and mountain  
581 topography, *Quat. Sci. Rev.*, 28, 977-990, 2009.

582 Lewkowicz, A. G. and Harris, C.: Frequency and magnitude of active-layer  
583 detachment failures in discontinuous and continuous permafrost, northern  
584 Canada, *Permafrost Periglac. Process.*, 16, 115-130, 2005.

585 Li, Q. Y. and Xie, Z. C.: Analysis on the characteristics of the vertical lapse rates of  
586 temperature. Taking Tibetan Plateau and its adjacent area as an example, *J*  
587 *Shihezi University (Natural Science)*, 24, 719-723, 2006 (In Chinese).

588 Liu, J. J., Cheng, Z. L., and Su, P. C.: The relationship between air temperature  
589 fluctuation and Glacial Lake outburst floods in Tibet, China, *Quat. Int.*, 321,  
590 78-87, 2014.

591 Liu, Y.: Research on the Typical Debris Flows Chain Based On RS in Palongzangbu  
592 Basin of Tibet, Master thesis, Chengdu University of Science And Technology,  
593 2013 (In Chinese).

594 Lu, R.R. and Li, D.J.: Ice-snow-melt debris flows in the Dongru Longba, Bomi  
595 county, Xizang, *J. Glaciol. Geocryol.*, 11, 148-160, 1989. (In Chinese).

596 McColl, S. T.: Paraglacial rock-slope stability, *Geomorphology*, 153–154, 1-16, 2012.

597 Noetzli, J., Gruber, S., Kohl, T., Salzmann, N., and Haeberli, W.: Three-dimensional  
598 distribution and evolution of permafrost temperatures in idealized  
599 high-mountain topography, *J. Geophys. Res.*, 112, F02S13, 2007.

600 Prancevic, J. P., Lamb, M. P., and Fuller, B. M.: Incipient sediment motion across the  
601 river to debris-flow transition. *Geology*, 42(3), 191-194, 2014.

602 Rahardjo, H., Leong, E. C., and Rezaur, R. B.: Effect of antecedent rainfall on  
603 pore-water pressure distribution characteristics in residual soil slopes under  
604 tropical rainfall, *Hydrol. Process.*, 22, 506-523, 2008.

605 Rango, A. and Martinec, J.: Revisiting the degree-day method for snowmelt  
606 computations, *JAWRA, J. Am. Water Resour. Assoc.*, 31, 657-669, 1995.

607 Recking A. Theoretical development on the effect of changing flow hydraulics on  
608 incipient bed load motion. *Water Resources Research*. 45,4, W04401, 2009.

609 Rengers, F.K., L.A. McGuire, J.W. Kean and D.E. Hobley, Model simulations of  
610 flood and debris flow timing in steep catchments after wildfire, *Water*  
611 *Resources Research*, 52, 8, 6041-6061, 2016.

612 Rist, A.: *Hydrothermal Processes within the Active Layer above Alpine Permafrost in*  
613 *Steep Scree Slopes and Their Influence on Slope Stability*, PhD Thesis, Swiss  
614 Federal Institute for Snow and Avalanche Research and University of Zurich,  
615 168 pp., 2007.

616 Ryzhkin, I. A. and Petrenko, V. F.: Physical mechanisms responsible for ice adhesion,  
617 *J. Phys. Chem. B*, 101, 6267-6270, 1997.

618 Sassa, K. and Wang, G. H., *Mechanism of Landslide-Triggered Debris Flows:*  
619 *Liquefaction Phenomena due to the Undrained Loading of Torrent Deposits.*  
620 *Debris-flow Hazards and Related Phenomena*, Springer, Berlin Heidelberg,  
621 81-104, 2005.

622 Sattler, K., Keiler, M., Zischg, A., and Schrott, L.: On the connection between debris  
623 flow activity and permafrost degradation: a case study from the Schnalstal,  
624 South Tyrolean Alps, Italy, *Permafrost Periglac. Process.*, 22, 254-265, 2011.

625 Schneuwly-Bollschweiler, M. and Stoffel, M.: Hydrometeorological triggers of  
626 periglacial debris flows in the Zermatt valley (Switzerland) since 1864, *J.*  
627 *Geophys. Res.*, 117, F02033, 2012.

628 Shang, Y. J., Yang, Z. F., Li, L., Liu, D. A., Liao, Q., and Wang, Y.: A super-large  
629 landslide in Tibet in 2000: background, occurrence, disaster, and origin,  
630 *Geomorphology*, 54, 225-243, 2003.

631 Springman, S. M., Jommi, C., and Teysseire, P.: Instabilities on moraine slopes  
632 induced by loss of suction: a case history, *Géotechnique*, 53, 3-10, 2003.

633 Stoffel, M. and Huggel, C.: Effects of climate change on mass movements in  
634 mountain environments, *Prog. Phys. Geog.*, 36, 421-439, 2012.

635 Stoffel, M., Bollschweiler, M., and Beniston, M.: Rainfall characteristics for  
636 periglacial debris flows in the Swiss Alps: past incidences-potential future  
637 evolutions, *Clim. Change*, 105, 263-280, 2011.

638 Takahashi, T., *Debris Flow: Mechanics, Prediction and Countermeasures*, CRC Press,  
639 Boca Raton, FL, 2014.

640 Takeuchi, Y., Kayastha, R. B., and Nakawo, M.: Characteristics of ablation and heat  
641 balance in debris-free and debris-covered areas on Khumbu Glacier, Nepal  
642 Himalayas, in the pre-monsoon season. *IAHS PUBLICATION*, 53-62, 2000.

643 The Ministry of Land and Resources P. R. C.: *China geological hazard*  
644 *Bulletin*(September edition), 2010.

645 Theule, J.I., Liebault, F., Loye, A., Laigle, D., and Jaboyedoff, M. Sediment budget  
646 monitoring of debris flow and bedload transport in the Manival Torrent, SE  
647 France. *Nat. Hazards Earth Syst. Sci.*, 12, 731-749, 2012.

648 Tognacca, C., Bezzola, G. R., and Minor, H. E.: Threshold criterion for debris-flow  
649 initiation due to channel bed failure, in: *Wieczoreck, G. F. (Ed.), Proceedings*  
650 *Second International Conference on Debris Flow Hazards Mitigation,*  
651 *Prediction and Assessment*, Taipei, 89-97, 2000.

652 Yang, W., Guo, X., Yao, T., Zhu, M. and Wang, Y.: Recent accelerating mass loss of  
653 southeast Tibetan glaciers and the relationship with changes in macroscale  
654 atmospheric circulations, *Clim. Dynam.*, 47, 805-815, 2016.

655 Yang, W., Yao, T., Xu, B., Ma, L., Wang, Z., and Wan, M.: Characteristics of recent  
656 temperate glacier fluctuations in the Parlung Zangbo River basin, southeast  
657 Tibetan Plateau, *Chin. Sci. Bull.*, 55, 2097-2102, 2010.

658 Yao, T.D., Thompson, L., Yang, W., Yu, W., Gao, Y., Guo, X., Yang, X., Duan, K.,  
659 Zhao, H., Xu, B., Pu, J., Lu, A., Xiang, Y., Kattel, D.B., and Joswiak, D.:  
660 Different glacier status with atmospheric circulations in Tibetan Plateau and  
661 surroundings, *Nat. Clim. Change*, 2, 663-667, 2012.

662 Yuan, G.X., Ding, R.W., Shang, Y.J., and Zeng, Q.L.: Genesis of the Quaternary  
663 accumulations along the Palong section of the Sichuan-Tibet Highway and

664 Their distribution regularities, *Geology and Exploration*, 48, 170-176, 2012 (In  
665 Chinese).  
666



667

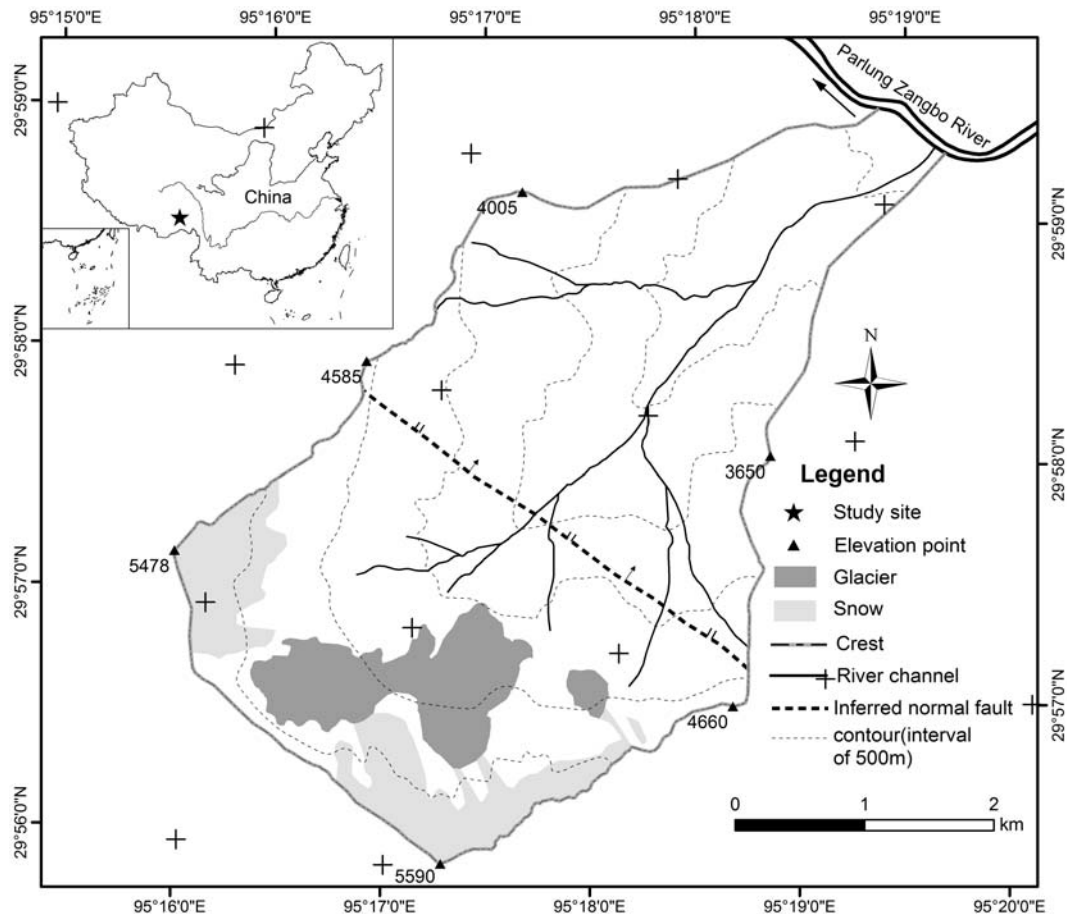
668 Table 1 Changes in glacier, snow, bare land, gully deposition and vegetation in Tianmo Valley

Year	Glacier (km <sup>2</sup> )	Glacier(eastern branch) (km <sup>2</sup> )	Snow (km <sup>2</sup> )	Bare land (km <sup>2</sup> )	Gully deposition (km <sup>2</sup> )	Vegetation (km <sup>2</sup> )
2000	1.77	0.16	2.13	2.80	0.44	10.46
2003	1.71	0.15	2.44	2.54	0.44	10.48
2006	1.53	0.12	2.68	2.44	0.44	10.55
2009	1.45	0.096	2.81	3.03	0.47	9.90
2013	1.42	0.088	1.74	3.83	0.51	10.17

669

670 Table 2 Basic information regarding the debris flows in Tianmo Valley and nearby valleys

No.	Name	Coordinates	Basin area (km <sup>2</sup> )	Glacier area (in 2006) (km <sup>2</sup> )	Date	Size class
1	Tianmo Valley	29°59'N 95°19'E	17.74	1.53	4 <sup>th</sup> Sep. 2007	6
					25 <sup>th</sup> Jul. 2010	5
					6 <sup>th</sup> Sep. 2010	5
2	Kangbu Valley	30°16'N 94°48'E	48.7	1.06	4 <sup>th</sup> Sep. 2007	3
3	Xuewa Valley	29°57'N 95°23'E	33.22	0.95	4 <sup>th</sup> Sep. 2007	2
4	Baka Valley	29°53'N 95°33'E	22.15	2.46	7 <sup>th</sup> Sep. 2007	3
5	Jiaqing Valley	30°16'N 94°49'E	15.51	1.12	9 <sup>th</sup> Sep. 2007	3



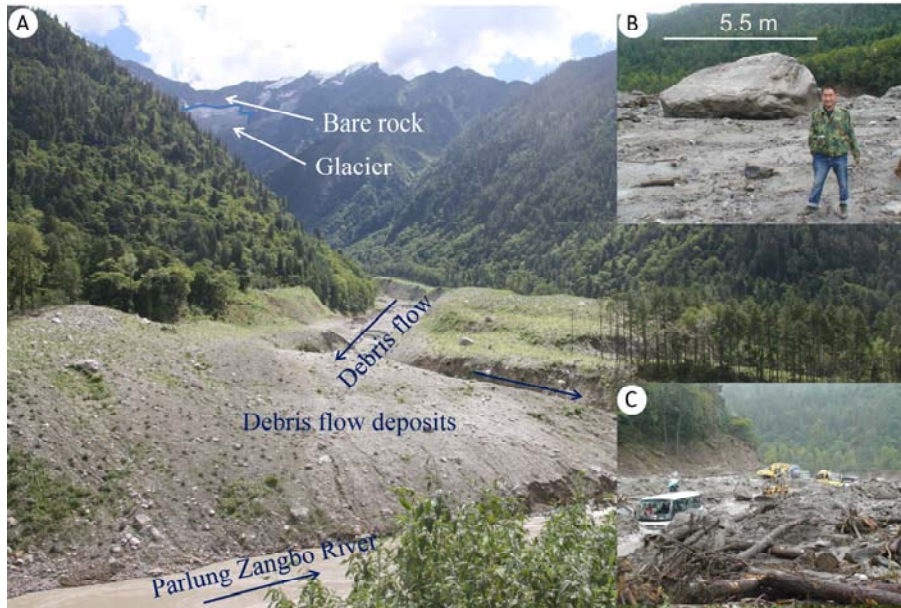
671  
672

Figure 1 Location of Tianmo Valley and related information



673  
674

Figure 2 Overview of the valley from the channel(in 2014)

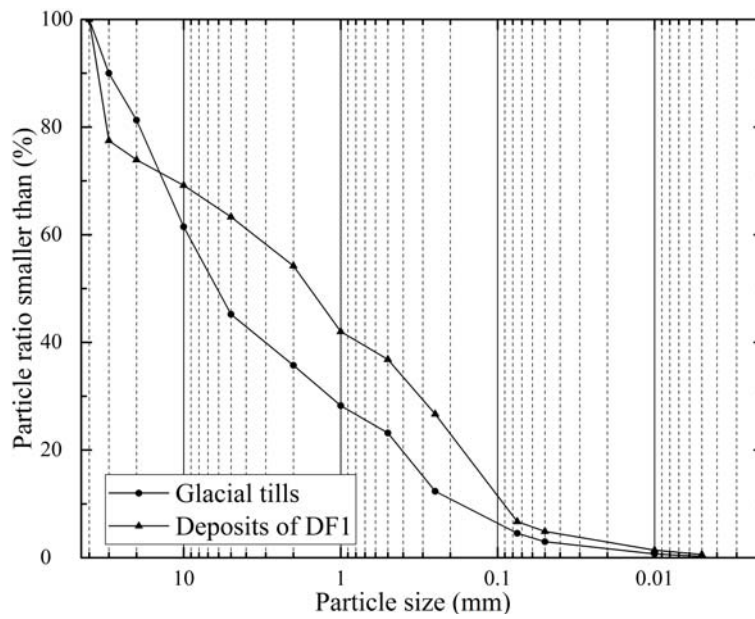


675

676 Figure 3 DF1 in 2007(A. Overview of the Tianmo debris flows from the downstream area; B& C.

677

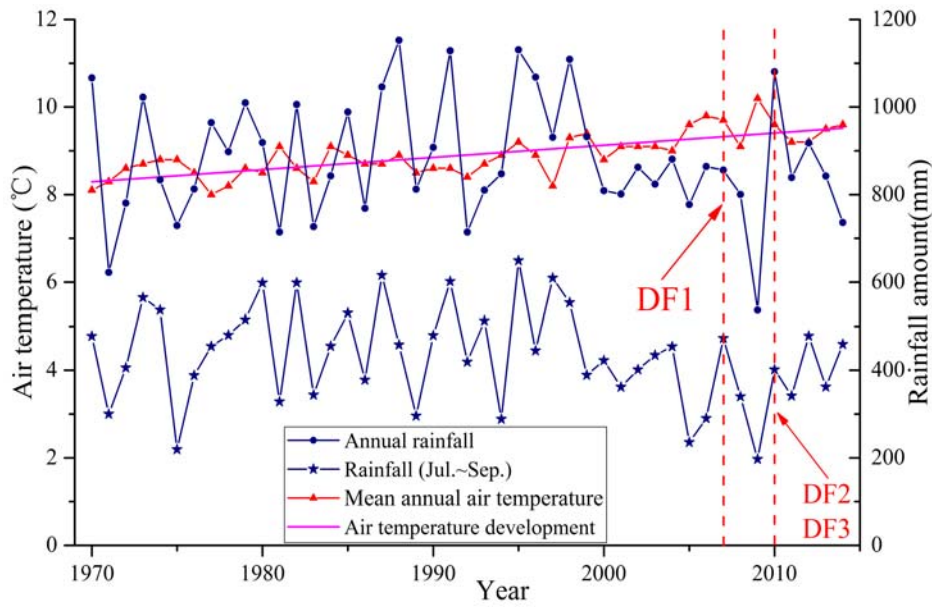
Boulder and debris flow deposits on the north side of the Parlung Zangbo River)



678

679

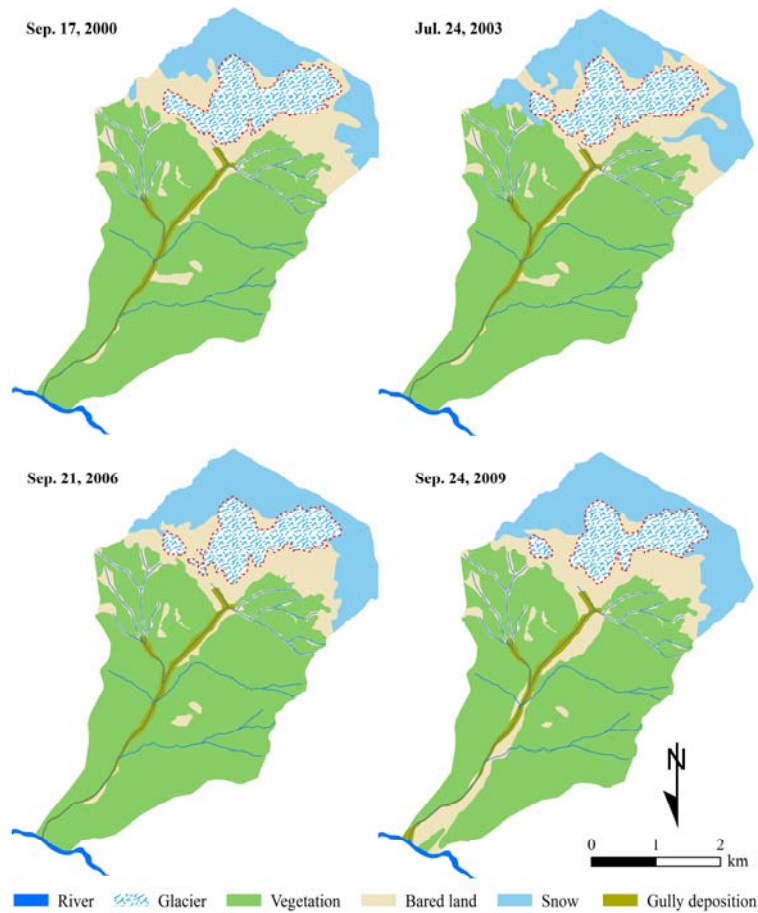
Figure 4 Particle size distributions of the glacial tills and debris flow deposits



680

681

Figure 5 Variation in the mean annual air temperature and rainfall at Bomi from 1970 to 2014



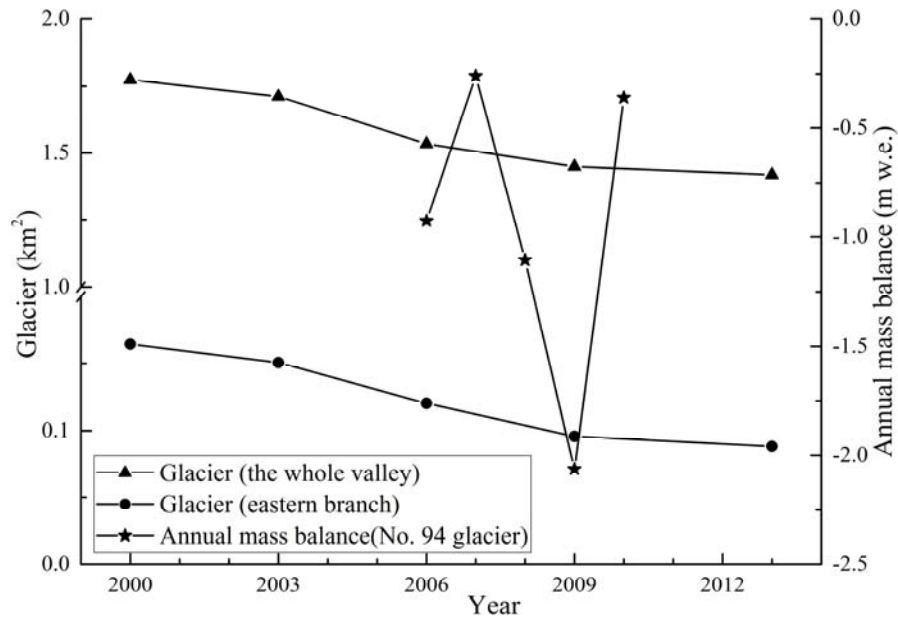
682

683

684

685

Figure 6 Distribution and changes in glacier, snow, bare land, gully deposition and vegetation in Tianmo Valley



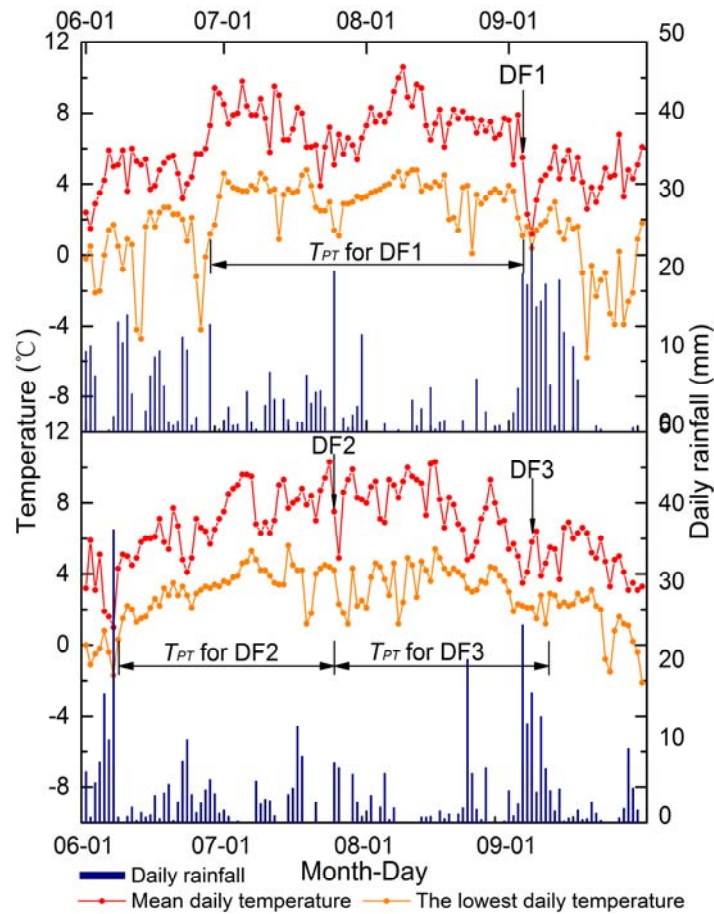
686

687

688

Figure 7 Changes in glacier over time and the measured annual mass balance of the Parlung No.

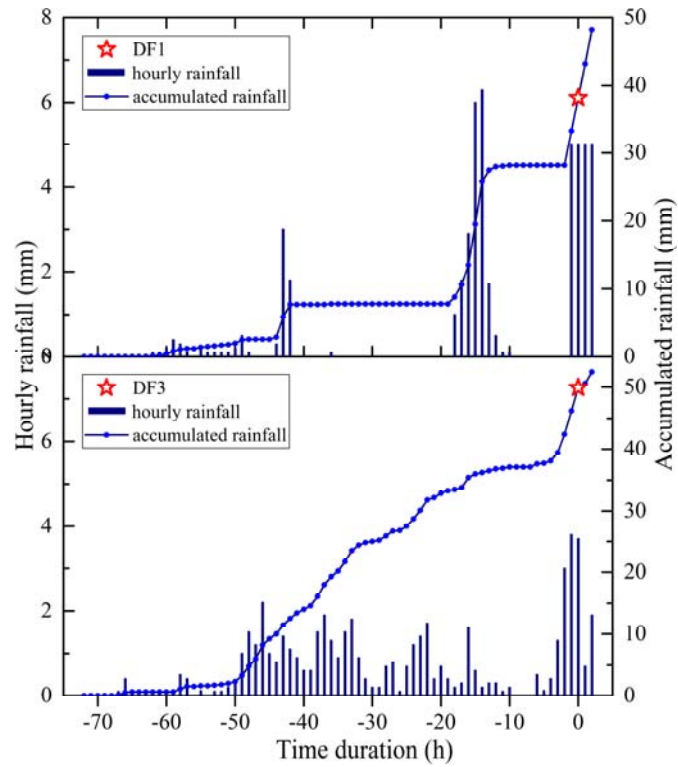
94 Glacier (mass balance was edited from Yang et al.(2015))



689

690

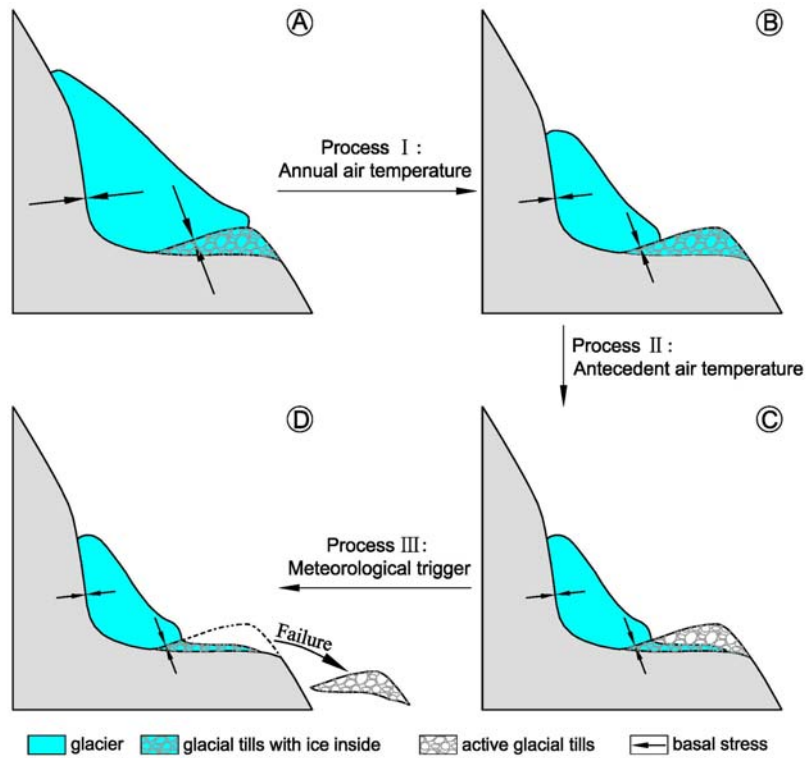
Figure 8 Air temperature and rainfall before and after DF1, DF2 and DF3



691

692

Figure 9 Variations in rainfall accumulation prior to DF1 and DF3 (no rainfall before DF2)



693

694 Figure 10 Changes in glacier and frozen glacial till before periglacial debris flow initiation(A:

695 glacial-covered glacial tills; B: uncovered and frozen glacial tills; C: active glacial tills; D: failure

696

of glacial tills)